

ISBN 978-88-95608-42-6; ISSN 2283-9216

VOL. 52, 2016 Guest Editors: Petar Sabev Varbanov, Peng-Yen Liew, Jun-Yow Yong, Jiří Jaromír Klemeš, Hon Loong Lam Copyright © 2016, AIDIC Servizi S.r.Í., DOI: 10.3303/CET1652073



# Fully Resolved CFD Simulation of a Hollow Fibre Membrane Module

Michael Harasek, Bahram Haddadi\*, Martin Miltner, Philipp Schretter, Christian Jordan

Technische Universität Wien, Institute of Chemical Engineering, Getreidemarkt 9/1662, 1060 Vienna, Austria bahram.haddadi.sisakht@tuwien.ac.at

Membrane processes play an important role in gas separation because they are robust and energy efficient. In the last decades a large number of studies have been carried out on this topic. Most of these studies were experimental, black box modelling or one-dimensional process modelling, but just a few applied Computational Fluid Dynamics (CFD) to have a more detailed look at these processes.

In addition to experimental investigation CFD can provide more detailed insights on the local flow, the concentration profiles which influence the equilibrium and the driving force for mass transfer without high costs, and lots of effort. Compared to black box modelling and process simulation CFD can also resolve all three spatial dimensions and this is valuable for the investigation of phenomena which are space dependent, e.g. local mixing in the membranes or concentration polarization.

In the current study a new CFD solver was developed. The new solver is based on the open source code OpenFOAM® for CFD modelling of membranes using solution-diffusion mechanism. It was validated and calibrated against processes simulation codes and also experiments.

The solver was used for the investigation of a geometrical parameter on the design of hollow fibre membrane modules. The effect of permeate outlet positioning (membrane module flow regime) on the quality of separation of a biogas mixture was carried out.

### 1. Introduction

Limited resources of fossil fuels and pollution caused by using these fuels, forces the world more towards extended utilization of alternative energy sources (Turner, 2004). One of the most promising sources of energy is biogas (Makaruk et al., 2010). Anaerobic digestion of organic materials is a sustainable way of biogas production (Pietrangeli et al., 2013). The desired products of this process (methane and hydrogen) are usually mixed with carbon dioxide. Removal of carbon dioxide from biogas products is known as biogas upgrading (Wu et al., 2015). Membranes have been applied successfully for biogas upgrading (Scott, 1995). There are different approaches for optimization of membrane designs, e.g. experimental studies (lab scale or pilot scale) or simulation approaches. Simulation methods provide a very good understanding of different phenomena at reasonably low time and cost manner. Among different simulation approaches Computational Fluid Dynamics (CFD) is a very powerful method, since besides temporal data it also provides spatial data in all directions. The full three dimensional discretization can give very good insight to the simulated process (e.g. analysis of mixing promoters like spacers and boundary layer effects like concentration polarization) and can also be used as a basis for validation of simpler and faster methods e.g. process simulation methods. Also the models and correlations which are derived by CFD simulations can be used in other simulation tools.

#### 2. Solution-diffusion mechanism

A very well established model for gas permeation through dense membranes is the solution-diffusion mechanism. This mechanism is divided into three main steps (Shao et al., 2009):

Sorption of the penetrants at the retentate side of the membrane

Please cite this article as: Harasek M., Haddadi B., Miltner M., Schretter P., Jordan C., 2016, Fully resolved cfd simulation of a hollow fibre membrane module, Chemical Engineering Transactions, 52, 433-438 DOI:10.3303/CET1652073

- Diffusion across the membrane
- Desorption at the permeate side

The whole mechanism is mathematically described by the relation between driving force and the mass flow rate across the membrane. The gas permeation driving force is connected to the partial pressure difference of the species at both sides of the membrane. The coefficient which is used for making the equality is known as permeance and shows the membrane ability to permeate the gas species. The formulation is as following:

$$J_i = \Pi_i(p_{i,0} - p_{i,l}) \tag{1}$$

 $J_i$  (Nm³/(s m²) is the specific flow rate of the species i through membrane,  $p_{i,0}$  (Pa) and  $p_{i,l}$  (Pa) are partial pressures of species i at feed and permeate side of membrane and the  $\Pi_i$  (Nm³/(s m² Pa) is the permeance of species i (Baker, 2000).

# 3. Computational Fluid Dynamics (CFD)

CFD is the analysis of systems by means of computer-based simulation involving fluid flow, mass transfer, heat transfer and etc. CFD codes are structured around the numerical algorithms that can tackle fluid flow problems with solving the following on computational grids. CFD simulations should be done in combination with good knowledge of the phenomena and underlying physics. In recent years, among available CFD packages, open source codes have received very special attention, because the source code is available for further development and implementations (and there is no requirement to pay license fees).

OpenFOAM® (OpenCFD Ltd., 2016) is a well-known open source CFD software which is published under GNU public license (Free Software Foundation Inc, 2016). The software is written in the programming language C++.Because of being object-oriented it provides programmers a very flexible structure for further developments.

#### 4. LTSMembraneFoam

Since there is no dedicated solver in OpenFOAM® for modelling semi-permeable membranes, the new solver LTSMembraneFoam was developed for this purpose. The new solver is capable of modelling a single phase multi-component flow in multi-layer membranes. The implemented membrane model is based on the solution-diffusion model and the solver can currently be used for modelling the membranes with zero thickness and multi-species permeation through the membrane.

Membranes usually operate at steady state conditions. Therefore, it is reasonable to simulate them also in steady state. The Local Time Stepping algorithm (LTS) was used in the solver for doing the calculations in steady state mode.

#### 5. Verification

After the development of a new solver it is always necessary to validate the solver. For validating the new LTSMembraneFoam the CFD simulation of the separation of a gas mixture in a hollow fibre module was compared to a process simulation code (Haddadi et al., 2015). In the next stage, the calibration of the new CFD tool was carried out. For calibrating the new CFD tool, the permeance of three different pure gases through the membrane using a hollow fibre module (PermSelect, PDMSXA – 10 cm²) were measured in the lab and compared with the values extracted from the simulation of the same module with the permeability data from module datasheet. The dimensions of the module can be seen in Figure 1. The module consists of 30 fibres and two outlets at the permeate side. The outlet close to the feed inlet is open and the other outlet is blocked for having a counter-current arrangement in the module.

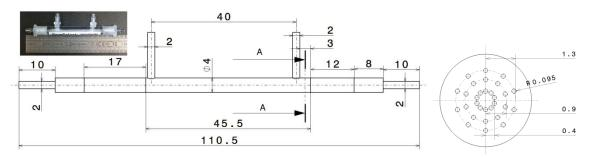


Figure 1: Membrane module and its dimensions

The properties for these different gases and the experimental operating conditions can be seen in Table 1. The simulations were also performed at the same conditions.

Table 1: Gases, module properties and operating conditions

Species	Permeability [Nm³ m/(s m²Pa)]	Retentate absolute pressure [Pa]	Permeate absolute pressure [Pa]	Operating temperature [K]
CO <sub>2</sub>	$2.44 \times 10^{-15}$	400,241	80,392	298
CH <sub>4</sub>	$7.13 \times 10^{-16}$	400,865	79,493	298
$H_2$	$4.88 \times 10^{-16}$	400,348	79,715	298

In Figure 2, the geometry prepared for being meshed, the inlet and outlets positions and also velocity vector plot at the permeate side for CO<sub>2</sub> can be seen.

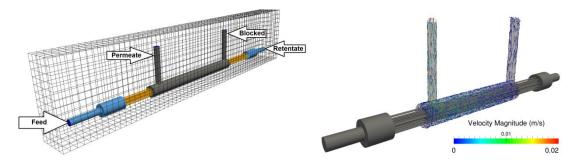


Figure 2: Module geometry and connections on the left hand side and velocity contour plots in the permeate side on the right hand side

The measured experimental results of the module for different gases can be seen in Table 2. In this table the feed flow rate, retentate flow rate and also the permeate flow rate for each gas are reported.

Table 2: Mass flows from lab experiments

Species	Feed flow [Nm³/s]	Retentate flow [Nm³/s]	Permeate flow [Nm³/s]	
CO <sub>2</sub>	$7.01 \times 10^{-6}$	6.91 × 10 <sup>-6</sup>	9.78 × 10 <sup>-8</sup>	
CH <sub>4</sub>	$7.74 \times 10^{-6}$	$6.94 \times 10^{-6}$	2.24 × 10 <sup>-8</sup>	
$H_2$	$6.19 \times 10^{-6}$	$5.24 \times 10^{-6}$	$2.16 \times 10^{-8}$	

The results from CFD simulations are listed in the Table 3. They are in an acceptable range but as it can be seen, there are some deviations in the results from the simulation and the experiments. These deviations between lab experiments and simulations are shown in Table 3 (in percentage). This can be justified with several reasons: the membrane is modelled as an ideal, homogeneous membrane (neglecting e.g. CO<sub>2</sub> influence on the material); the inaccuracy of the measurement devices used in the experimental measurements and the not exact permeabilities in the module data sheet (Schretter, 2016).

Table 3: Mass flows from CFD simulations

Species	Feed flow	Retentate flow	Permeate flow	
	[Nm <sup>3</sup> /s]	[Nm <sup>3</sup> /s]	[Nm <sup>3</sup> /s]	
CO <sub>2</sub>	6.94 × 10 <sup>-6</sup> (1 %)	6.92 × 10 <sup>-6</sup> (0.1 %)	8.38 × 10 <sup>-8</sup> (14 %)	
CH <sub>4</sub>	$7.34 \times 10^{-6} (5 \%)$	$7.35 \times 10^{-6} (6 \%)$	1.88 × 10 <sup>-8</sup> (16 %)	
$H_2$	$5.72 \times 10^{-6} (8 \%)$	$5.71 \times 10^{-6} (9 \%)$	1.89 × 10 <sup>-8</sup> (13 %)	

# 6. Geometry

Next, a hollow fibre module with different outlet positioning at the permeate side was modelled to get the different flow configurations in the module and to investigate its effects on the module separation performance. For this purpose, a simplified module with a length of 0.5 m and 7 fibres with a diameter of 0.001 m was simulated. The module has five outlets at the permeate side (the distance between two neighbouring outlets is

0.1 m) and depending on the configuration one outlet is open and the rest are closed. The module can be seen in Figure 3. Table 4 shows the investigated geometries based on the permeate outlet position. The mesh and geometry were created using commercial tool Ansys GAMBIT®.

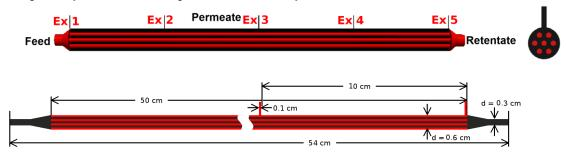


Figure 3: Module permeate outlets (scaled 1:10 in the length direction) and module dimensions

Table 4: Case ID based on the permeate outlet investigated

Case	Case 1	Case 2	Case 3	Case 4	Case 5
Permeate outlet	Ex 1	Ex 2	Ex 3	Ex 4	Ex 5
(Figure 3)	100 %		50/50		100 %
	counter-current				co-current

#### 7. Simulation conditions

All simulations were performed applying the same conditions except for the active outlet at the permeate side. The feed was biogas and it consists of  $CO_2$ ,  $CH_4$  and  $O_2$  with respective mass fractions of 0.58, 0.406 and 0.012. The feed entered the module at an absolute pressure of 9 bar and temperature of 316.5 K with a mass flow rate of  $6.2 \times 10^{-6}$  kg/s. The absolute pressure at the permeate outlet was kept constant at 1.1 bar. The species permeances for the selected type of membrane are as following (Makaruk et al. 2010):

- $CO_2:5.91 \times 10^{-5} \text{ m}^3/(\text{m}^2 \text{ bar s})$
- $CH_4:1.59 \times 10^{-6} \text{ m}^3/(\text{m}^2 \text{ bar s})$
- $O_2:1.36 \times 10^{-5} \text{ m}^3/(\text{m}^2 \text{ bar s})$

## 8. Data extraction and representation

For all the cases the data for retentate and permeate side were extracted between the lines AB (retentate side) and CD (permeate side) according to Figure 4. Since the module length is rather big compared to the module diameter, it is hard to visualize result plots (contour plots). Therefore, all plots are scaled with the scale factor 1:10 (Figure 4). For sake of space just the contour plots for case 3 are shown in this paper. Case 3 was selected because it is a combination of both co and counter-current flows and the effect of both can be seen in the same contour plot.

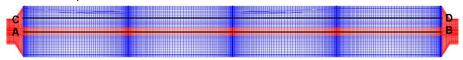


Figure 4: Data extraction lines on the scaled geometry in the length direction (scale 1:10)

#### 9. Results

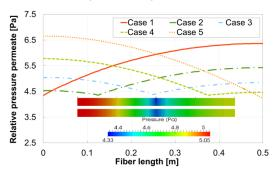
Different flow properties can be extracted from the CFD simulations carried out. In here three characteristic key properties were extracted and evaluated:

- Pressure
- CO<sub>2</sub> mass fraction
- Overall CO<sub>2</sub> mass flow

# 9.1 Pressure

As mentioned before, in the solution-diffusion mechanism the partial pressure of each component is the driving force and plays an important role in the amount of mass passing through the membrane. Species

partial pressure is a function of species mass fraction and total pressure, so it is important to have a closer look at the pressure distribution at both sides of membrane. Figure 5 shows the relative pressure along the module length for permeate side is shown. As it can be seen, the lowest pressure occurs at the outlet for all the cases as expected. According to Eq(1), however the pressure in the permeate side is lower (at constant retentate pressure and species mass fractions) the driving force is bigger. It can be seen in Figure 5, that case 3 has the lowest average pressure on permeate side. If all other conditions are kept equal it is expected that it has the highest driving force and consequently highest trans-membrane mass flow.



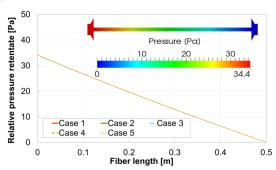


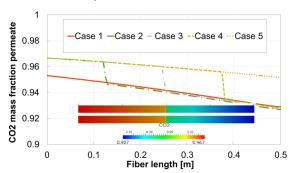
Figure 5: Permeate pressure profile along module length

Figure 6: Retentate pressure profile along module length

In Figure 6 the pressure drop in the retentate side is plotted against module length. The shell side pressure drop is close to 35 Pa for all the cases and the pressure profile is very close to linear.

#### 9.2 CO2 mass fraction

At the permeate side in all the cases  $CO_2$  mass fraction decreases moving from the feed side to the retentate side (Figure 7). Figure 7 also shows that the  $CO_2$  mass fractions are higher in the counter-current part for all the cases. Moving the permeate outlet from the end of the module to the beginning of the module (from case 5 to case 1) the  $CO_2$  mass fraction at the outlet is also increasing. This means a higher purity of  $CO_2$  in the counter-current operation of the module can be achieved.



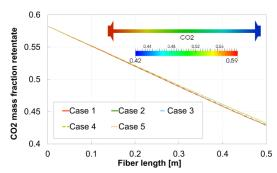


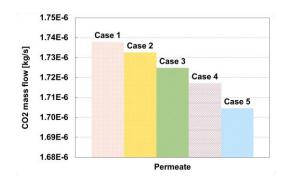
Figure 7: Permeate CO<sub>2</sub> mass fraction profile along module length

Figure 8: Retentate CO<sub>2</sub> mass fraction profile along module length

Figure 8 shows the  $CO_2$  mass fractions at the retentate side along the fibre length. As it can be seen, the  $CO_2$  mass fraction decreases for all cases along the length from feed to the retentate. The slope of the decrease in  $CO_2$  mass fraction gets bigger by moving the permeate outlet from the end of the module (close to retentate outlet) to the beginning of the module (feed inlet). This means, by shifting the membrane operation configuration from co-current to counter-current, the mass fraction of  $CO_2$  in the retentate outlet decreases (more pure product).

#### 9.3 Overall CO2 mass flow

Figure 9 shows the  $CO_2$  mass flow for different cases. As it can be seen, that case 1 (counter-current case) has the highest  $CO_2$ mass flow at the permeate outlet compare to the other cases. As expected, Figure 10 also confirms the same behaviour for  $CO_2$  mass flow at the retentate outlet, by moving from a co-current configuration to a counter-current configuration less  $CO_2$  is going out from retentate outlet.



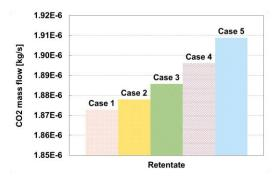


Figure 9: CO2 mass flow at the permeate outlet

Figure 10: CO2 mass flow at the retentate outlet

#### 10. Conclusion

A new CFD membrane investigation tool based on the open source code OpenFOAM® was developed. The new tool is capable of modelling membrane modules resolved in temporal and spatial dimensions. It was validated and calibrated against process simulation codes and also experimental measurements. As a simple example, the effect of a geometric design parameter (position of retentate outlet) on the performance of a hollow fiber membrane module for biogas purification was investigated. As it is also shown in this study using this CFD solver (LTSMembraneFoam) can provide a good detailed view in the phenomenon that cannot be investigated using process simulation tools and can be used for deriving models to be used in the other simulation tools (models for considering different phenomena e.g. mixing in the membranes or concentration polarization).

#### Reference

Baker R.W., 2000, Membrane technology, Encyclopedia of Polymer Science and Technology. 3, John Wiley & Sons, Inc., New Jersey, United States, DOI: 10.1002/0471440264.pst194.

Haddadi Sisakht B., Jordan C., Schretter P., Lassmann T., Harasek M., 2015, Designing Better Membrane Modules Using CFD. Chemical Product and Process Modeling, 11(1), 57-66, DOI: 10.1515/cppm-2015-0066.

Makaruk A., Miltner M., Harasek M., 2010, Membrane biogas upgrading processes for the production of natural gas substitute, Separation and Purification Technology, 74(1), 83-92, DOI: 10.1016/j.seppur.2010.05.010.

OpenCFD Ltd., 2016, OpenCFD Ltd., <www.openfoam.org>, accessed 12.04.2016.

Pietrangeli R., Lauri P.B., Bragatto P.A., 2013, Safe Operation of Biogas Plants in Italy, Chemical Engineering Transactions, 32, 199-204, DOI: 10.3303/CET1332034.

Schretter P., 2016, Simulation of membrane modules with OpenFOAM®, Vienna University of Technology (Master thesis), Vienna, Austria.

Scott K., 1995, Handbook of industrial membranes, Elsevier, Amsterdam, Netherlands, ISBN: 978-1-85617-233-2.

Shao L., Low B.T., Chung T.S., Greenberg A.R., 2009, Polymeric membranes for the hydrogen economy: contemporary approaches and prospects for the future, Journal of Membrane Science, 327(1), 18-31, DOI: 10.1016/j.memsci.2008.11.019.

Stallman R., 1993, Using and porting GNU CC (Vol. 675), Free Software Foundation, <www.gnu.org>, accessed 12.04.2016.

Turner J.A., 2004, Sustainable hydrogen production, Science, 305(5686), 972-974, DOI: 10.1126/science.1103197.

Wu B., Zhang X., Xu Y., Bao D., Zhang S., 2015, Assessment of the energy consumption of the biogas upgrading process with pressure swing adsorption using novel adsorbents, Journal of Cleaner Production, 101:251-61, DOI: 10.1016/j.jclepro.2015.03.082.